Efficiency prediction for a low head bulb turbine with SAS SST and zonal LES turbulence models

D Jošt, A Škerlavaj

Turboinštitut d.d., Rovšnikova 7, 1000 Ljubljana, Slovenia

E-mail: dragica.jost@turboinstitut.si

Abstract A comparison between results of numerical simulations and measurements for a 3-blade bulb turbine is presented in order to determine an appropriate numerical setup for accurate and reliable simulations of flow in low head turbines. Numerical analysis was done for three angles of runner blades at two values of head. For the smallest blade angle the efficiency was quite accurately predicted, but for the optimal and maximal blade angles steady state analysis entirely failed to predict the efficiency due to underestimated torque on the shaft and incorrect results in the draft tube. Transient simulation with SST did not give satisfactory results, but with SAS and zonal LES models the prediction of efficiency was significantly improved. From the results obtained by SAS and zonal LES the interdependence between turbulence models, vortex structures in the flow, values of eddy viscosity and flow energy losses in the draft tube can be seen. Also the effect of using the bounded central differential scheme instead of the high resolution scheme was evident. To test the effect of grid density, simulations were performed on four grids. While a difference between results obtained on the basic grid and on the fine grid was small, the results obtained on the coarse grids were not satisfactory.

1. Introduction

For turbines with small pressure head, such as Kaplan and especially bulb turbines, an accurate simulation of flow in a draft tube is more important for accuracy of efficiency prediction than for Francis turbines. In years 1999, 2001 and 2005 three workshops "Turbine-99" were performed with the aim to gain the knowledge how to perform trustworthy simulations of Kaplan draft tubes. The experimental data was provided for a local best efficiency point, which was close to the best efficiency of the system. The inlet conditions were provided from experimental measurements by the laser Doppler velocimetry (LDV) method. For all tested RANS models, including the SST model, the predicted secondary flow was too weak [1]. The best results were obtained by Kurosawa and Nakamura [2] using the dynamic Smagorinsky LES model. Apart from the Turbine-99 workshops, some other published results outlined the problem of accurate predictions in Kaplan and bulb turbines. In a review paper [3] a steady-state prediction of efficiency of an axial turbine with the SST model was presented. The discrepancy between numerical and experimental values was increasing with rise of runner blade angle. Up to some point, the results were improved by mesh refinement in guide vane cascade and runner, because the original mesh was rather coarse with large values of y^+. In a recent paper [4] about numerical simulations of a Kaplan turbine it was reported that steady state results obtained by various turbulence models (k-ε, k-ω, BSL, SST, SSG RSM) were very poor, while unsteady simulations considerably improved the accuracy of efficiency prediction. The best results were achieved using the zonal LES model, but even the prediction with the transient SST simulation was much better than the steady-state SST simulation. The influence of head on numerical predictions

for bulb turbines is shown in [5]. At low head the inaccuracy is larger, especially at large runner blade angles and large discharge values.

The purpose of this paper is to extend the conclusions for Kaplan turbines presented in [4] to bulb turbines and to check the influence of mesh refinement and the effect of the advection scheme on the results. The accuracy of numerical prediction is most critical at low head and therefore a 3-blade bulb turbine which operates at extremely low head was chosen as a test case.

2. Turbulence models and discretisation schemes

In [4] steady state analysis was done with several RANS turbulence models, such as the standard k-ε turbulence model, the Wilcox k-ω model, the Baseline (BSL) k-ω model, the SST model and the ε-based SSG RSM [6]. The best results, which were still rather poor at large discharge values, were obtained with SST and SSG RSM. The results obtained with SSG RSM were no better than the results of SST. In this paper steady state analysis was done only with SST. For transient simulations besides SST, two scale-resolving simulation models (SAS SST and ZLES) were used. In [4] positive effects of curvature correction (CC) and Kato-Launder limiter of production term (KL) on accuracy of results were found, therefore both, CC and KL, were used in all simulations presented in this paper.

In the simulations, we used either 'high resolution' or the bounded central difference scheme. The high-resolution scheme is a bounded second order upwind biased discretisation. The scheme calculates the bounded values based on the procedure of the Barth and Jespersen's scheme [7, 8]. The bounded central difference scheme (BCDS) is based on the normalised variable diagram and blends from the CDS scheme to the first-order upwind scheme when the convection boundedness criterion [9] is violated. For time discretisation a second order backward Euler scheme was used.

For convenience, in this paper short labels are used for turbulence models and discretisation schemes: SST for the Shear Stress Transport model, SAS for the SAS SST model, ZLES for the SAS SST with zonal LES in the draft tube, HRS for the High Resolution Scheme and BCDS for the bounded Central Differential Scheme.

3. Efficiency prediction for a low head bulb turbine

Results of a detailed numerical analysis of flow in a low head bulb turbine, carried out with the commercial solver ANSYS CFX, Version 14.0, are presented. A model of the turbine was tested on a test rig at Turboinštitut, in accordance with international standard IEC 60193 [10]. Numerical simulations were at first performed at ψ_{BEP}, then a detailed research was done at even smaller head (see table 1), where accurate prediction of flow in the draft tube is even more important for accurate efficiency prediction.

The turbine consists of an inlet part with a vertical pier, 16 guide vanes, 3-blade runner and a draft tube. Tip clearance was modelled while hub clearance was neglected. Based on a study [11] it can be assumed that the effect of hub clearance on the prediction of turbine efficiency is much smaller than the influence of the runner blade tip gap.

Table 1: Local best efficiency operating points (LBEP) for two values of ψ

Operating point	β (deg.)	φ/φ_{BEP}	ψ/ψ_{BEP}
OP1	12	0.73	0.97
OP2	20	1.00	0.97
OP3	28	1.30	0.97
OP4	12	0.66	0.61
OP5	20	0.96	0.61
OP6	28	1.29	0.61

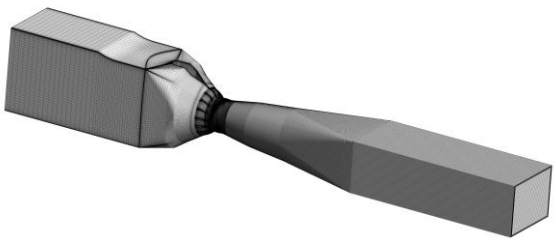

Figure 1: Computational grid

Grids in all parts were structured. Most of the simulations were done on a basic grid (BG) with about 9 million nodes. Some simulations were done on a fine grid (FG) with 35 million nodes, a

coarse grid (CG) with 5.3 million nodes and a very coarse grid (VCG) with 2.1 million nodes. The basic computational grid can be seen in figure 1, while numbers of nodes in all computational grids are presented in table 2.

The numerical analysis was done in three stages. Firstly, a steady state analysis for three angles of runner blades and two values of energy coefficient ψ was performed. Secondly, a transient analysis was done with three turbulence models using two discretisation schemes (SST HRS, SAS HRS, SAS BCDS and ZLES BCDS) at only one operating point. At this stage the effect of grid density was tested. Finally, a transient analysis was performed at several operating points for three angles of runner blades and two values of energy coefficient, with the ZLES turbulence model and BCDS for advection term on the basic grid.

Table 2: Number of nodes in all turbine parts for basic, very coarse, coarse and fine grids

	Grid label	Inlet part	Guide vane cascade	Runner	Draft tube	Draft tube prolongation	Total number of nodes
Basic grid	BG	1,394,720	2,059,568	2,076,603	1,936,188	1,573,336	9,040,415
Very coarse grid	VCG	223,375	1,032,976	531,603	211,428	170,332	2,169,714
Coarse grid	CG	223,375	1,032,976	531,603	1,936,188	1,573,336	5,297,478
Fine grid	FG	1,394,720	2,059,568	2,076,603	16,324,636	13,176,576	35,032,103

3.1 Steady state analysis

True transient interaction between stator and rotor can be predicted only by transient rotor stator simulation. Unfortunately, such simulations are very time consuming and they require large computer resources. For steady state analysis, a frozen rotor or a stage condition is prescribed between stationary parts and runner. With frozen rotor model the two frames of reference (stationary and rotating) are connected in such a way that they each have a fixed relative position throughout the calculation. The frozen rotor model is most useful when the circumferential variation of the flow is large relative to the component pitch. The disadvantage of this model is that the transient effects at the frame change interface are not modelled. No mixing between stationary and rotating components is taken into account. An alternative to the frozen rotor is a stage condition. The stage averaging at the frame change interface is equivalent to assuming that the physical mixing supplied by the relative motion between components is sufficiently large to cause any upstream velocity profile to mix out prior to entering the downstream machine component. Stage analysis is not appropriate when the circumferential variation of the flow is significant [6].

In our case, the guide vane cascade was close to the runner and due to the wakes behind the vanes circumferential variation of flow was significant. Therefore the frozen rotor model was quite suitable at the frame change interface between the guide vanes and the runner. At the interface between the runner and the draft tube the mixing supplied by the runner motion was significant, but not sufficiently intensive to mix out the wakes behind the runner blades. In figure 2 it can be seen that both models, frozen rotor and stage, introduced errors at the inlet of the draft tube. By frozen rotor a bit stronger wakes than by transient rotor stator were obtained behind the runner blades. Besides, contrary to reality, the positions of the wakes remained fixed during the simulation. The circumferential averaging of the stage model looks even less realistic. Steady state simulations were performed with both, stage and frozen rotor conditions at the interface between the runner and the draft tube.

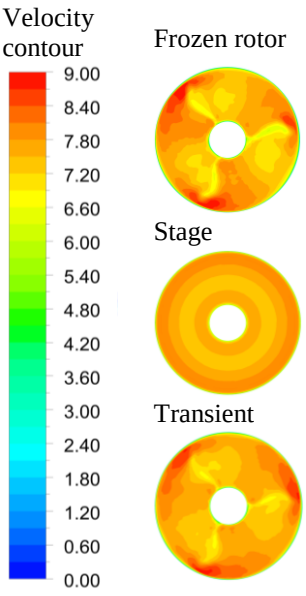

Figure 2: Velocity distribution at the draft tube inlet obtained by frozen rotor, stage and transient stator rotor at OP6

Steady state analysis was done with SST turbulence model on the basic grid. For discretisation of the advection term, the 'high resolution' scheme (HRS) implemented in ANSYS-CFX was used. The input data were geometry, head and rotational speed. Values of discharge, torque on the shaft, flow energy losses and efficiency were calculated from numerical results. Converged steady state solutions were not obtained, mostly due to unsteadiness in the draft tube. Flow energy losses in the draft tube and consequently also the values of discharge, torque and efficiency oscillated during the simulations. Therefore, instead of the values of the last iteration the averaged values of last 300 iterations were used as a result of steady state analysis. Steady state simulations were done for three angles of runner blades at two values of energy coefficient ($\psi/\psi_{BEP} = 0.97$ and $\psi/\psi_{BEP} = 0.61$). Results for the local best efficiency points are presented in table3.

In figure 3 flow in the draft tube at OP4, OP5 and OP6 ($\psi = 0.61\psi_{BEP}$) is presented. It can be seen that due to the frozen rotor condition strong wakes behind the runner blades caused swirls in the draft tube. At the outlet part of the draft tube, where conical shape changed into a shape with rectangular cross-section, the swirls enlarged and at OP6 they even joined in to one huge swirl. Flow energy losses increased drastically and at OP6 they exceeded 13.4% of head. With the stage condition, losses in the draft tube are significantly smaller. Consequently, calculated discharge, torque on the shaft and efficiency values are larger than when the frozen rotor condition was used. Calculated values of torque on the shaft were smaller than the measured ones. In case of the stage condition the largest discrepancy in torque is about 5%, but in case of frozen rotor condition with increasing blade angles the discrepancy increased. At OP3 and OP6 it reached 10.3% and 14.5%, respectively. For both, stage and frozen rotor conditions, calculated efficiency values are smaller than the measured ones. In case of frozen rotor condition the discrepancy in efficiency at OP3 and OP6 exceeded 10% and 14%, respectively, while in case of stage condition it is less than 4.5%. It can be concluded that numerical prediction of efficiency by steady state analysis with frozen rotor condition entirely failed due to underestimated torque on the shaft and overestimated losses in the draft tube. Results obtained with the stage condition are closer to the measured values but with more than 4% difference they are also not acceptable. At OP6 where the discrepancy was the largest, a steady state simulation with frozen rotor condition was repeated on the fine grid (FG), but no improvement of results was achieved.

Table 3: Comparison of steady state numerical results at LBEP with measurements

	frozen rotor condition				stage condition			
	Q_{CFD}/Q_{Exp}	M_{CFD}/M_{Exp}	$H_{DT}/H*100$	η_{CFD}/η_{Exp}	Q_{CFD}/Q_{Exp}	M_{CFD}/M_{Exp}	$H_{DT}/H*100$	η_{CFD}/η_{Exp}
OP1	1.026	0.993	3.67	0.972	1.027	1.001	1.95	0.984
OP2	1.010	0.949	5.35	0.951	1.011	0.949	4.08	0.959
OP3	0.999	0.897	11.33	0.900	1.016	0.972	4.30	0.959
OP4	1.028	0.993	2.88	0.969	1.028	0.994	2.19	0.972
OP5	0.973	0.880	7.71	0.915	1.006	0.964	3.27	0.962
OP6	0.997	0.855	13.44	0.860	1.004	0.955	4.16	0.955

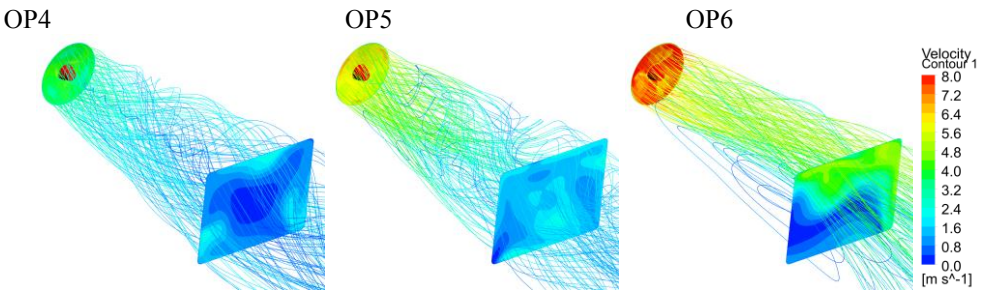

Figure 3: Flow in the draft tube at local best efficiency points for blade angles 12, 20 and 28 deg., $\psi/\psi_{BEP} = 0.61$, steady state results, frozen rotor condition, basic grid (BG)

3.2 Transient analysis at one operating point

At OP6 (the LBEP for runner blade angle 28 deg., $\psi/\psi_{BEP} = 0.61$) the discrepancy between numerical and measured results was the largest. Therefore, this point was chosen for transient simulations performed with SST, SAS and the ZLES models on the basic grid (BG). In combination with the SST model HRS was used for the advection term, while in combination with the SAS and the ZLES models BCDS was used. In order to see the effect of the advection scheme the simulation with the SAS model on BG was repeated with HRS. To see whether the results can be additionally improved by grid refinement the simulations with the SAS and the ZLES were repeated on fine grid. The purpose of simulations on more coarse grids was to see whether it was possible to reduce the CPU time without too significant effect on accuracy of results. Values of y^+ for different grids are presented in table 4.

For simulations on BG and FG time step corresponded to 0.5 deg. of runner revolution while for CG and VCG it corresponded to 1 deg. of runner revolution. Maximal values of Courant number in the draft tube were less than 4.4 while averaged values were less than 0.1 for all cases. The simulations run on a supercomputer cluster with 512 Quad-Core Intel Xeon processors L5335. For all employed combinations of turbulence models, advection schemes and grid density, CPU is presented in table 5.

Table 4: Averaged values of y^+ for different grids, simulations at OP6 with SAS BCDS

Model/Grid	VCG	CG	BG	FG
Inlet part	55	55	5.7	5.7
Guide vanes	7	7	3	3
Runner	23	23	5	5
Draft tube	148	16	14	9

Table 5: CPU (in hours) for transient simulations on 64 cores, 1 runner revolution

Model/Grid	VCG	CG	BG	FG
SST HRS			20.33	
SAS HRS			22.66	
SAS BCDS	3.97	6.73	22.13	68
ZLES BCDS	4.03		22.60	70

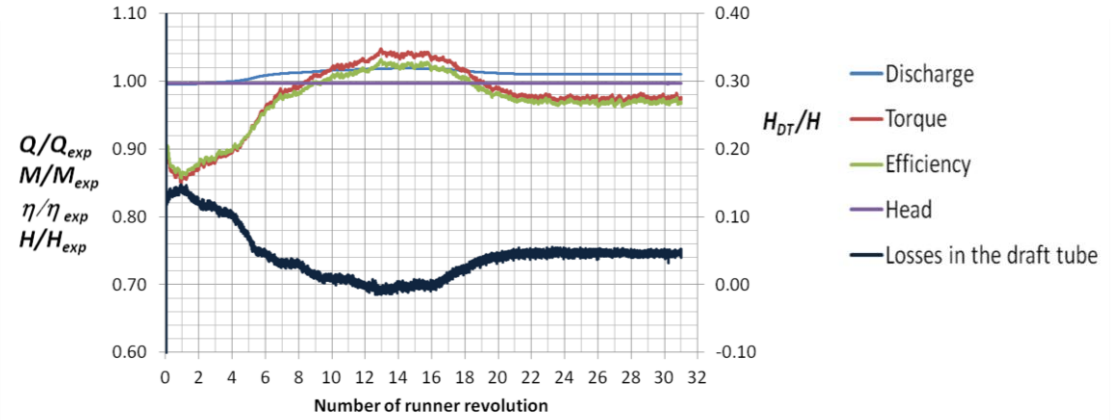

Figure 4: Values of discharge, head, torque, losses in the draft tube and turbine efficiency during transient simulation with ZLES model on the basic grid at OP6

Typical evolution of results obtained with ZLES or SAS is presented in figure 4. Transient simulations started from the results of the steady state simulation. During the first 14 runner revolutions flow energy losses in the draft tube were decreasing and consequently the values of discharge, torque and efficiency were increasing. A large swirl (see figure 3, OP6) at the right part of the draft tube (looking in the flow direction) obtained by the steady state analysis was moving towards the outlet and became smaller and smaller. The values of discharge, torque on the shaft and efficiency were increasing when flow energy losses in the draft tube were decreasing and vice versa. The head was input data and it was constant during the simulation. All observed quantities stabilized after 20 runner revolutions. Only small oscillation due to unsteadiness of the flow remained. On the contrary, the results of transient simulation with the SST model on BG after 33 runner revolutions still did not stabilize.

In figure 5 flow in the draft tube visualized by streamlines and velocity distribution on inlet and outlet of the draft tube is presented for three turbulence models (SST, SAS, ZLES), two advection schemes (BCDS and HRS) and different grids (BG, FG, VCG). In case of the SST model a lot of swirls in the flow remained and velocity distribution at the draft tube outlet is not uniform. During simulations with the SAS and the ZLES models on BG most of the swirls in the flow vanished. Velocity distribution at the draft tube outlet is quite uniform. No effect of additional grid refinement (FG) on streamlines and velocity distribution at the draft tube outlet can be seen. A negative effect of grid coarsening was considerable, especially in case of SAS on VCG, where large swirls in the draft tube can be observed. Hardly any difference can be seen between flow obtained with SAS HRS and SAS BCDS.

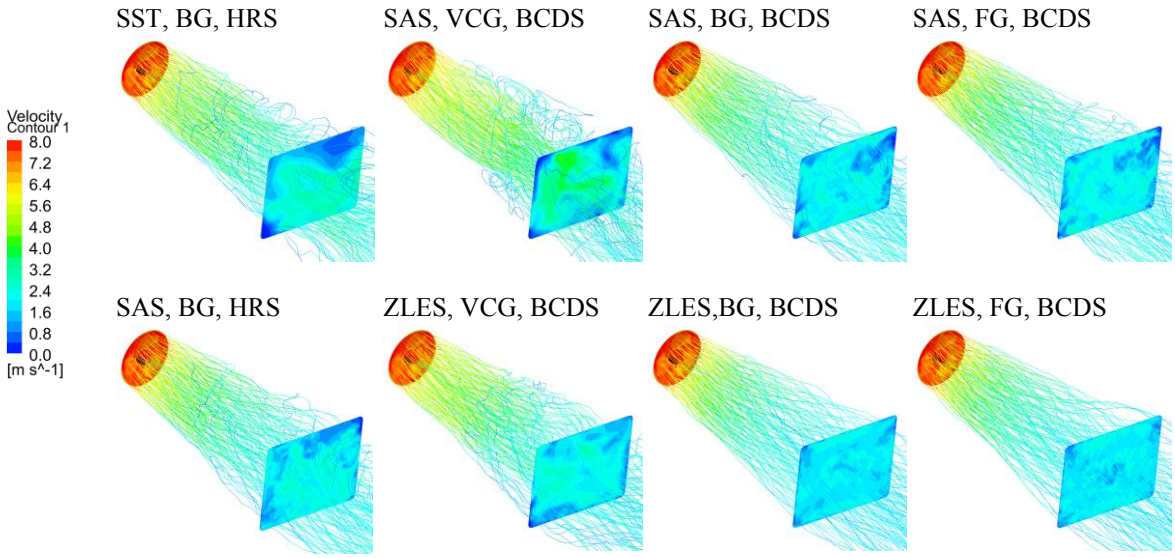

Figure 5: Flow in the draft tube visualized by streamlines and velocity contours at the draft tube inlet and outlet at OP6, results of transient simulations after 31 runner revolutions

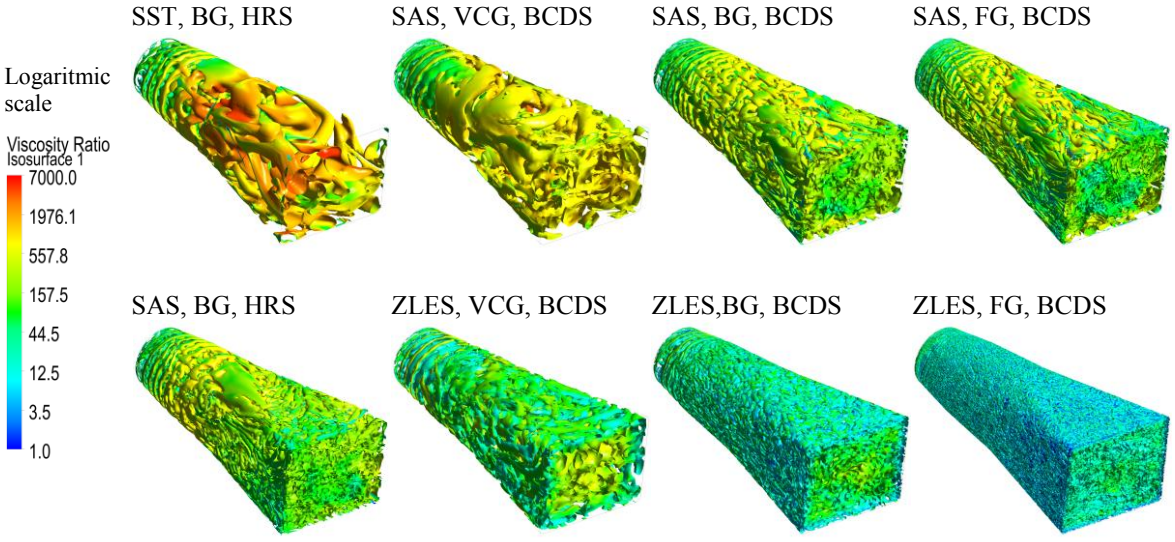

Figure 6: Vortical structures in the draft tube visualized by iso-surfaces of velocity invariant $Q = 0$ at OP6, results of transient simulations after 31 runner revolutions

Vortical structures in the flow are presented by iso-surfaces of second invariant of velocity gradient Q (Q = 0) coloured by viscosity ratio (Eddy Viscosity / Dynamic Viscosity) in figure 6. The differences due to a choice of turbulence model and grid density are significant. With the SST model only large vortical structures were obtained and a value of viscosity ratio was high. With the SAS model also smaller structures in the flow were obtained, the value of viscosity ratio was smaller. Very fine structures were well resolved with the ZLES model where the value of viscosity ratio was the smallest. In case of the SAS model by additional grid refinement (FG) no improvement was achieved, the differences in vortical structures and in values of viscosity ratio were negligible. On the contrary, the grid refinement did have a positive effect on results obtained with the ZLES model. Even finer structures in the flow were obtained and viscosity ratio was smaller. Contrary to expectations, a transient simulation with the ZLES model on VCG gave much better results than SAS on VCG and even than SAS on CG. In fact, the results obtained by ZLES on VCG looked more like the results of SAS on BG than like the results of SAS on VCG.

In figure 7 all results of steady state and transient simulations at OP6 are compared to each other and to the measurements. The influence of grid density, turbulence model and advection scheme on predicted values of discharge, torque on the shaft, flow energy losses and efficiency can be seen. Flow energy losses were divided by head. Discharge, torque and efficiency values were divided by the measured values at the same operating point. For results of a steady state simulation with frozen rotor condition on both frame change interfaces, a label SFF is used. When at the interface between the runner and the draft tube the stage condition was prescribed, a label SFS is used. A label T referenced to transient results. Labels HRS and BCDS referenced to high resolution scheme and bounded central differential scheme for the advection term. So a label BG,SFF,SST,HRS means steady state results obtained with frozen rotor on BG with the SST model and HRS used for the advection term, while FG,T,ZLES,BCDS means transient results on fine grid with the ZLES model and BCDS.

For transient analysis the values during the last 5 runner revolutions were averaged. The results of transient simulation with the SST model after 33 runner revolutions still did not stabilize, but it was clearly seen that flow energy losses in the draft tube were larger and efficiency was at least 2% lower than the values obtained with the SAS and the ZLES models. Although the results of SST were not stabilised, their averaged values are presented in diagrams in figure 7.

For all simulations at OP6 the discrepancy between calculated and measured values of discharge was in the range of 1%. All simulations underestimated values of torque on the shaft. Drastic discrepancy of more than 14% in case of steady state results with frozen rotor condition reduced to the smallest discrepancy of 1.76% in case of transient simulation with ZLES BCDS on FG.

Flow energy losses before the runner were between 2.69% and 3.05% of head. A difference between losses obtained with SAS HRS and SAS BCDS indicated the effect of advection scheme. When the same turbulence model and the same scheme (SAS BCDS) were used, larger losses were obtained on CG and VCG.

Flow energy losses in the runner were between 6.4% and 8.38% of head. The highest value was obtained by steady state simulation with the stage condition. Losses in the runner decreased when BCDS was used instead of HRS. The smallest losses in the runner were obtained on CG and VCG because tip clearance was not modelled.

Losses in the draft tube obtained by steady state simulations with the stage condition are 4.16% of head while in case of frozen rotor they exceeded 13.4% on BG and even increased to 14.7% on FG. With transient simulations losses in the draft tube decreased significantly, their values were on BG between 4.5% (SAS BCDS and ZLES BCDS) and 5.6% (SST HRS) of head. Additional grid refinement didn`t have any effect on losses in case of the SAS model, but with the ZLES model on FG the smallest losses, equal to 3.94% of head, were obtained. Comparing the losses obtained on BG with SAS HRS and SAS BCDS the latter were smaller for 1.1% of head. In spite of the same grid in the draft tube, calculated flow energy losses obtained on CG were much larger than those obtained on BG. Clearly too coarse grid in the runner without tip clearance affected the flow at the draft tube inlet and consequently in the whole draft tube. The results on VCG were even worse.

SAS BCDS and ZLES BCDS on BG predicted nearly the same value of efficiency, a difference to the measurement was 3%. In case of SST the discrepancy to the measured value was 5%. The efficiency value obtained by SAS on BG with BCDS was for 1.8% higher than the value obtained by the same turbulence model on the same grid, but with HRS. The higher efficiency value was obtained due to smaller flow energy losses in all turbine parts and higher torque on the shaft. In case of the SAS model by additional grid refinement (FG) the calculated value of efficiency was not improved. On the contrary, in case of the ZLES model grid refinement resulted in 0.44% higher value of efficiency. Due to significantly larger flow energy losses on CG and VCG the efficiency values were much smaller. A transient simulation with the ZLES model on VCG gave much better results than SAS on VCG and even than SAS on CG. Nevertheless, predicted value was still about 6% smaller than the measured one and 3% smaller than the value calculated on BG.

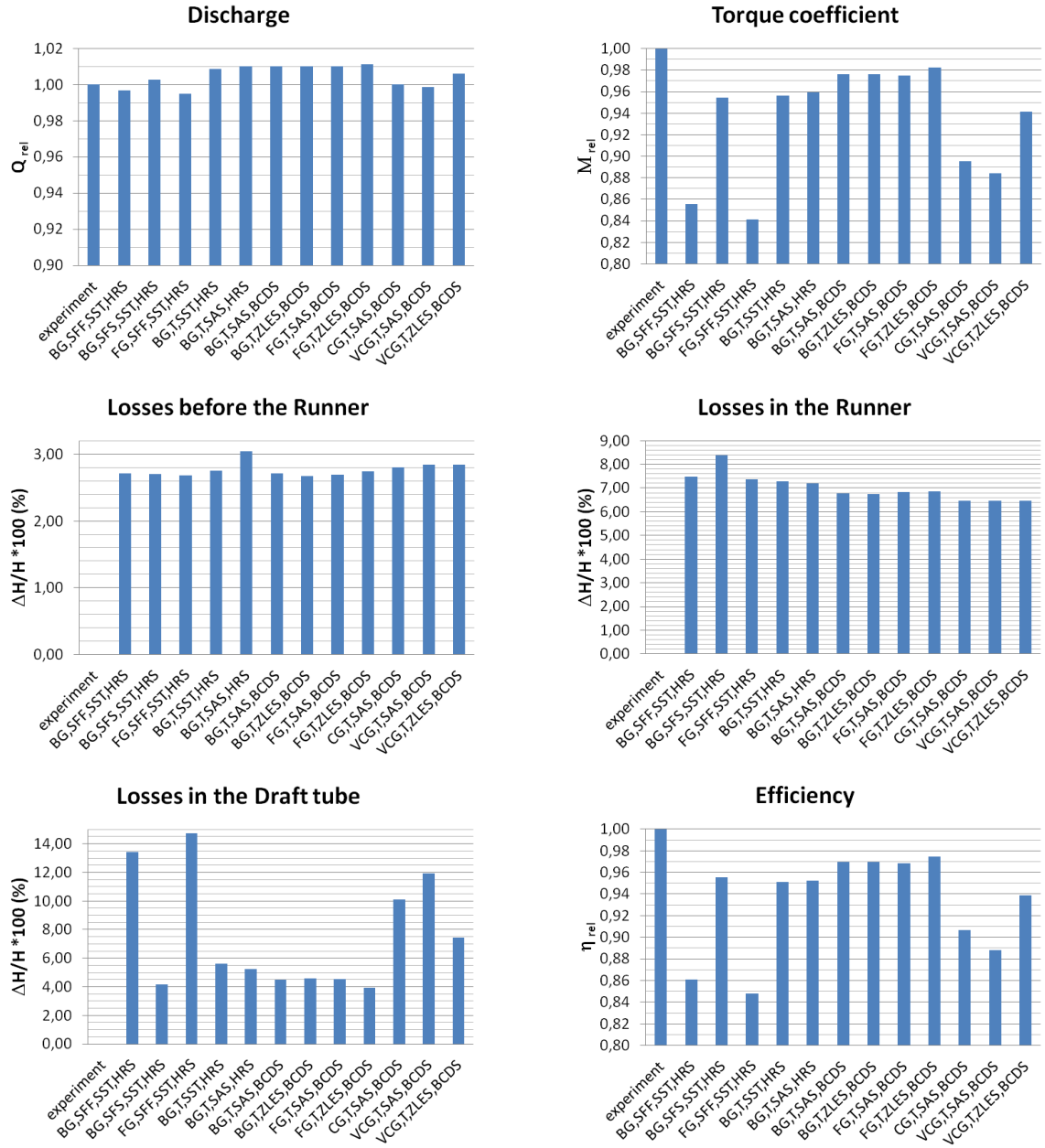

Figure 7: Comparison of numerical results at OP6 obtained by SST, SAS and ZLES on different grids to the measurements

3.3 Transient simulations for different operating regimes

Transient simulations with ZLES BCDS were performed on the basic grid for both values of energy coefficient (ψ/ψ_{BEP} = 0.97 and ψ/ψ_{BEP} = 0.61). Such simulations are very time consuming therefore complete efficiency curves were not obtained. In figure 8 the efficiency values were divided by measured efficiency value at the best efficiency point. For all operating points the accuracy of efficiency prediction was improved in comparison to the steady-state results. An improvement for blade angle 12 deg. was small, but for angles 20 and 28 deg. it was considerable. The discrepancy between measured and numerical results for ψ/ψ_{BEP} = 0.97 at LBEP for blade angles 12, 20 and 28 deg. were 0.2%, 0.56% and 1.5% respectively. For smaller head (ψ/ψ_{BEP} = 0.61) the discrepancy at LBEP for blade angles 12 deg., 20 deg. and 28 deg. were 2.5%, 1.9% and 2.7%, respectively.

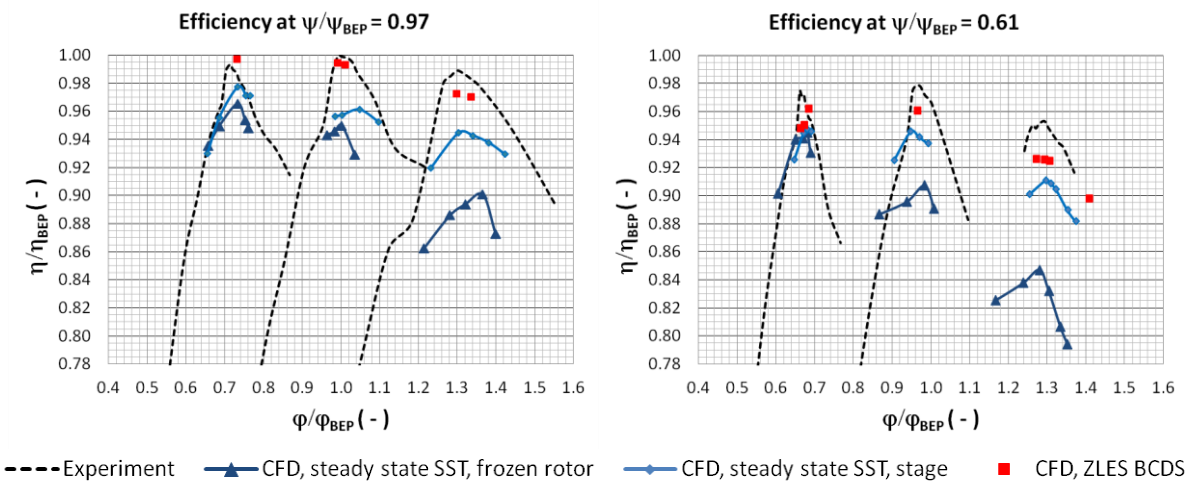

Figure 8: Comparison of predicted efficiency to the experimental values

4. Conclusions

On the basis of a detailed analysis of flow in a bulb turbine with different turbulence models and at different operating regimes it can be concluded:

- Steady state analysis with the frozen rotor condition between the runner and the draft tube entirely failed to predict turbine efficiency due to underestimated torque on the shaft and especially overestimated flow energy losses in the draft tube. With the stage condition the results were closer to the measured values but still not satisfactory.
- Transient simulations with the SST, the SAS and the ZLES models were performed at one operating point for maximal runner blade angle at the smaller value of head. Results of transient simulation with the SST model were still not reliable but with the SAS and especially with the ZLES models large improvement was achieved. On the basic grid the results of SAS and ZLES were equally accurate, but on very coarse and fine grids the results of the ZLES model were significantly better. Comparing the results of SAS HRS and SAS BCDS it can be seen that agreement with measurements is better when BCDS was used due to smaller losses and better prediction of torque on the shaft.
- Comparing the results of the steady state analysis and the results of the ZLES model to the measurements, the agreement of the latter one was better at all operating regimes. At BEP the discrepancy between results of the ZLES model and measured values was 0.56%, but for the smaller head (ψ/ψ_{BEP} = 0.61) in spite of large improvement the discrepancy was even on the fine grid still about 2.5%.
- Too long CPU time is main disadvantage of transient simulations and the reason for their limited use in design process. It can be expected that with future development of hardware and software the problem will be overcome.

Acknowledgements
The authors are grateful to the colleagues and especially to the head of Turbine R & D Department Dr. Vesko Djelić, for geometrical data and measured results.
The research was partially funded by Slovenian Research Agency ARRS, Contract No. P2-0196 and Contract No. 1000-09-130263.

References

[1] Cervantes M J, Engström T F, Gustavsson L H 2005 "Proceedings of Turbine-99 III". Luleå University of Technology, number 2005:20
[2] Kurosawa S, Nakamura K 2005 Unsteady turbulent flow simulation in Turbine-99 draft tube, In *Proc. of the Turbine-99 III Workshop on Draft Tube Flow*, (Porjus, Sweden, 8-9 December 2005) Luleå University of Technology, 2005:20, ISSN:1402-1528
[3] Jošt D, Lipej A, Mežnar P 2008 *N*umerical Prediction of Efficiency, Cavitation and Unsteady Phenomena in Water Turbines, *Proceedings of the 9th Biennial ASME Conference on Engineering Systems Design and Analysis, ESDA08,* July 7-9, 2008, Haifa, Israel
[4] Jošt D, Škerlavaj A, Lipej A 2012 Numerical flow simulation and efficiency prediction for axial turbines by advanced turbulence models. *IOP Conference Series: Materials Science and Engineering, vol. 15, no. 6, p. 062016 (9 p.).*
[5] Gehrer A, Benigni H, Köstenberger M 2004 Unsteady Simulation of the Flow Through a Horizontal-Shaft Bulb Turbine, *22nd IAHR Symposium on Hydraulic Machinery and Systems,* Stockholm, Sweden.
[6] *ANSYS (2014).* ANSYS CFX-Solver Theory Guide. *Ansys Inc., Canonsburg, Pennsylvania, USA.*
[7] Barth T J, Jespersen D C 1989 The design and application of upwind schemes on unstructured meshes. *27th Aerospace Sciences Meeting, AIAA Paper 89-0366, 12 p.*
[8] Darwish M S, Moukalled F 2003 TVD Schemes for Unstructured Grids. *International Journal of Heat and Mass Transfer, vol. 46, no. 4, p. 599-611.*
[9] Jasak H, Weller H G, Gosman A D 1999 High resolution NVD differencing scheme for arbitrarily unstructured meshes. *International Journal for Numerical Methods in Fluids, vol. 31, no. 2, 431–449.*
[10] *IEC 60193 (1999).* Hydraulic turbines, storage pumps and pump-turbine – Model acceptance tests. *International Electrotechnical Commission. Geneva, Switzerland.*
[11] Guénette V, Houde S, Ciocan G D, Dumas G, Huang J, Deschênes C (2012), Numerical prediction of a bulb turbine performance hill chart through RANS simulations. *IOP Conference Series: Earth and Environmental, Volume 15, Part 3.*

Nomenclature

Variables and quantities:

g		Gravity
H		Head
H_{DT}	$H_{DT} = \Delta P_{tot}/(\rho g)$	Losses in the draft tube
M		Torque on the shaft
P_{tot}		Total pressure
Q		Discharge
r		Runner radius
β		Runner blade angle
ρ		Density
η		Efficiency
φ	$\varphi = Q/(\pi\omega r^3)$	Discharge coefficient
ψ	$2gH/(\omega r)^2$	Energy coefficient
ω		Runner speed

Indekses:

CFD	CFD value
Exp	Experimental value

Abbreviations:

BCDS	Bounded Central Differential Scheme
BEP	Best Efficiency Point
BG	Basic Grid
CG	Coarse Grid
FG	Fine Grid
HRS	High Resolution Scheme
LBEP	Local Best Eff. Point
VCG	Very Coarse Grid